Inhibition of ammonia monooxygenase from ammonia oxidising archaea by linear and aromatic alkynes

Chloë L. Wright[a], Arne Schatteman[a], Andrew T. Crombie[a], J. Colin Murrell[b], Laura E. Lehtovirta-Morley[a]#

[a]School of Biological Sciences, University of East Anglia, Norwich, United Kingdom

[b]School of Environmental Sciences, University of East Anglia, Norwich, United Kingdom

Running title: Inhibition of the ammonia monooxygenase by alkynes

#Address correspondence to: Laura E. Lehtovirta-Morley, l.lehtovirta-morley@uea.ac.uk

Keywords: Ammonia monooxygenase; ammonia oxidisers; methanotroph; inhibition; linear 1-alkynes; phenylacetylene

Abstract

Ammonia monooxygenase (AMO) is a key nitrogen transforming enzyme belonging to the same copper-dependent membrane monooxygenase family (CuMMO) as the particulate methane monooxygenase (pMMO). The AMO from ammonia oxidising archaea (AOA) is very divergent from both the AMO of ammonia oxidising bacteria (AOB) and the pMMO from methanotrophs and little is known about the structure or substrate range of the archaeal AMO. This study compares inhibition by C_2-C_8 linear 1-alkynes of AMO from two phylogenetically distinct strains of AOA, "*Candidatus* Nitrosocosmicus franklandus" C13 and "*Candidatus* Nitrosotalea sinensis" Nd2, with AMO from *Nitrosomonas europaea* and pMMO from *Methylococcus capsulatus* (Bath). An increased sensitivity of the archaeal AMO to short-chain-length alkynes ($\leq C_5$) appeared to be conserved across AOA lineages. Similarities in C_2-C_8 alkyne inhibition profiles between AMO from AOA and pMMO from *M. capsulatus* suggested that the archaeal AMO has a narrower substrate range compared to that of *N. europaea* AMO. Inhibition of AMO from "*Ca.* Nitrosocosmicus franklandus" and *N. europaea* by the aromatic alkyne phenylacetylene was also investigated. Kinetic data revealed that the mechanism by which phenylacetylene inhibits "*Ca.* Nitrosocosmicus franklandus" and *N. europaea* is different, indicating differences in the AMO active site between AOA and AOB. Phenylacetylene was found to be a specific and irreversible inhibitor of AMO from "*Ca.* Nitrosocosmicus franklandus" which does not compete with NH_3 for binding at the active site.

45 **Importance**

46 Archaeal and bacterial ammonia oxidisers (AOA and AOB) initiate nitrification by
47 oxidising ammonia to hydroxylamine, a reaction catalysed by ammonia monooxygenase (AMO).
48 AMO enzyme is difficult to purify in active form and its structure and biochemistry remain
49 largely unexplored. The bacterial AMO and the closely related particulate methane
50 monooxygenase (pMMO) have a broad range of hydrocarbon co-oxidation substrates. This study
51 provides insights into the AMO of previously unstudied archaeal genera, by comparing the
52 response of the archaeal AMO, a bacterial AMO and pMMO to inhibition by linear 1-alkynes
53 and the aromatic alkyne, phenylacetylene. Reduced sensitivity to inhibition by larger alkynes
54 suggests that the archaeal AMO has a narrower hydrocarbon substrate range compared to the
55 bacterial AMO, as previously reported for other genera of AOA. Phenylacetylene inhibited the
56 archaeal and bacterial AMO at different thresholds and by different mechanisms of inhibition,
57 highlighting structural differences between the two forms of monooxygenase.

58

59

60

61

62

63

64

65

66 **Introduction**

67 Nitrification is a key microbial process in the global nitrogen cycle. Autotrophic archaeal
68 and bacterial ammonia oxidisers (AOA and AOB, respectively) and comammox bacteria, which
69 carry out the complete oxidation of ammonia to nitrate (1, 2), initiate nitrification through the
70 oxidation of ammonia (NH_3) to hydroxylamine (NH_2OH), a reaction catalysed by ammonia
71 monooxygenase (AMO). The AMO is the only enzyme of the ammonia oxidation pathway
72 which is shared by all three major groups of ammonia oxidisers (3). Quantitative assessments
73 based on the *amoA* gene, which encodes the AmoA subunit of the AMO, have revealed that
74 AOA are ubiquitous in the environment and are among the most numerous living organisms on
75 Earth, often outnumbering AOB in many environments where nitrification occurs (4-7).
76 Environmental surveys using *amoA* as a marker gene have been crucial for our understanding of
77 the distribution and diversity of AOA; however, little is known about the structure or
78 biochemistry of the archaeal AMO and how this differs from that of AOB.

79 The AMO is a copper-dependent multimeric transmembrane enzyme belonging to the
80 CuMMO superfamily which comprises ammonia, methane and alkane monooxygenases (7-9).
81 Members of the CuMMO family have a broad substrate range and it has been suggested that
82 subsequent metabolic steps define the functional role of microbes containing CuMMO (10, 11).
83 For example, the AOB *Nitrosomonas europaea* and *Nitrosococcus oceani* can oxidise methane
84 but lack necessary downstream enzymes to gain reducing power from methane oxidation (12,
85 13). Likewise, the particulate methane monooxygenase (pMMO) of methanotrophs can co-
86 oxidise NH_3, (14-16) as well as various hydrocarbons, for instance linear 1-alkanes (C_2-C_5) and
87 alkenes (C_2-C_4) (17-19), and halogenated hydrocarbons (20), but none of these oxidation
88 substrates can support growth. The bacterial AMO has a broader substrate range than the pMMO

and is capable of co-oxidising 1-alkanes (C_2-C_8) and alkenes (C_2-C_5) (21), halogenated hydrocarbons (22, 23), aromatic compounds (24) and sulfides (25, 26) to yield hydroxylated products. Difficulties in purifying active AMO limit the amount of structural data available and many predictions about the structure of AMO are based on homology to the pMMO (8, 10, 27, and 28). However, the pMMO itself has proven challenging to fully characterise, and the nature and location of the site of O_2 activation and methane oxidation remains uncertain. To date, a diiron site located on the PmoC subunit (29), and multiple copper sites of different nuclearities located on separate subunits (PmoA, PmoB and PmoC) have all been suggested as potential active sites (27, 30-34).

Insights regarding the structure and function of the AMO have largely come from whole cell studies investigating its interaction with both reversible and irreversible inhibitors. For example, the bacterial AMO is inhibited by the copper chelator allylthiourea (ATU) which strongly indicates that it is a copper-dependent enzyme (18, 35-38). Acetylene is a well characterised inhibitor of both the AMO and pMMO (39-41). With *N. europaea*, acetylene acts as a suicide substrate and cells require *de novo* protein synthesis of new AMO to re-establish NH_3 oxidising activity (42). Incubations with ^{14}[C]-acetylene resulted in the covalent radiolabelling of *N. europaea* AMO, enabling identification of the genes coding for AMO (41, 43). A subsequent study found that the ketene product of acetylene activation bound covalently to a histidine residue (H191) in the AmoA subunit of *N. europaea*, a residue thought to be in the proximity of the AMO active site (44). While acetylene is also an irreversible inhibitor of the archaeal AMO, the AMO from archaea lack the histidine residue responsible for binding in *N. europaea*, suggesting that the product of acetylene oxidation must bind at a different position on the enzyme. AMO from *N. europaea* is also irreversibly inhibited by other terminal and sub-

terminal alkynes including C_3-C_{10} 1-alkynes (21), 3-hexyne (45) and 1,7-octadiyne (46). Interestingly, in *N. europaea*, the degree of inhibition by 1-alkynes, as a function of chain length, inversely mirrors the activity with the corresponding 1-alkanes (21).

Virtually nothing is known about the substrate range of the archaeal AMO. Previously, Taylor *et al.,* (47, 48) showed that, in whole cell studies, aliphatic *n*-alkynes (C_2-C_9) differentially inhibited bacterial and archaeal AMOs, with the AOA being less sensitive to $\geq C_5$ 1-alkynes. Inhibition of AMO by 1-octyne (C_8) has since been used in environmental and mesocosm studies to discriminate between the contributions of AOA and AOB to soil nitrification (49-52). A field study by Im *et al.,* (53) showed that the abundance of archaeal *amoA* genes decreased when the soil was treated with the aromatic alkyne phenylacetylene, although the effects of phenylacetylene on pure cultures of AOA were not investigated. Phenylacetylene was shown to be a strong inhibitor of the AMO from *N. europaea* (41), with complete inhibition at <1 µM (54) and the AMO from *N. europaea* is capable of oxidising aromatic compounds including the alkane analogue of phenylacetylene, ethylbenzene (24, 55). Interestingly, the oxidation of aromatic hydrocarbons has not been observed for the pMMO (17, 21, 40, and 56).

The initial aim of this study was to undertake a comprehensive assessment of the inhibition of archaeal AMO activity by C_2-C_8 linear 1-alkynes using two terrestrial AOA strains from distinct thaumarchaeal lineages, "*Candidatus* Nitrososocosmicus franklandus" C13 and "*Candidatus* Nitrosotalea sinensis" Nd2. 1-alkyne inhibition profiles of *N. europaea* AMO and the pMMO from *Methylococcus capsulatus* (Bath) were also investigated for comparison. For consistency and to provide a direct comparison with the AMO, the inhibition of NH_3-oxidising activity by the pMMO from *M. capsulatus* (Bath) was investigated. NH_3 is a co-metabolic

134 substrate of the pMMO from *M. capsulatus* (Bath) and is oxidised to hydroxylamine, which is
135 further oxidised to produce NO_2^- (14, 57).

136 Next, phenylacetylene inhibition profiles of NH_3 oxidation by "*Ca.* Nitrosocosmicus
137 franklandus" and *N. europaea* cells were compared. The kinetic mechanism of inhibition of
138 intact cells of "*Ca.* Nitrosocosmicus franklandus" and *N. europaea* by phenylacetylene was
139 investigated to explore differences in the biochemistry of the archaeal and bacterial AMO.
140 Evidence from previous studies suggests that NH_3, rather than ammonium (NH_4^+), is the growth
141 substrate oxidised by the bacterial AMO (58), but the preferred substrate (NH_3/NH_4^+) oxidised by
142 the archaeal AMO has not been determined. However, it is highly likely to also be NH_3 based on
143 archaeal and bacterial AMO sequence comparisons (59). At the pH of the systems used here, the
144 majority of the NH_3 (pK_a of 9.25) would be protonated. Therefore, calculations of kinetic
145 parameters presented in this study are based on total reduced inorganic nitrogen ($NH_3 + NH_4^+$) as
146 the substrate.

147

148 **Materials and Methods**

149 **Materials.** Phenylacetylene (98%), propyne, 1-pentyne, 1-hexyne, 1-heptyne and 1-
150 octyne (C_3, C_5, C_6, C_7 and C_8 linear 1-alkynes, ≥97%) were obtained from Sigma-Aldrich (now
151 Merck). 1-Butyne was supplied by Apollo Gases Ltd. Acetylene was obtained from BOC, a
152 member of the Linde Group. Protein concentrations were determined using a Pierce BCA protein
153 assay kit (Thermo Scientific) as described by the manufacturer.

154 **Growth of cultures. "***Candidatus* Nitrosotalea sinensis" Nd2 and "*Candidatus*
155 Nitrosocosmicus franklandus" C13 (60, 61) were grown as follows: "*Ca.* Nitrosocosmicus

franklandus" was cultivated in freshwater medium (FWM) buffered with 10 mM HEPES (pH 7.5) and supplemented with 4 mM NH_4Cl as previously described (61). The acidophilic AOA "*Ca.* Nitrosotalea sinensis" was cultivated in FWM buffered with 2.5 mM MES (pH 5.3) and supplemented with 400 µM NH_4Cl as previously described (60). Both "*Ca.* Nitrosocosmicus franklandus" and "*Ca.* Nitrosotalea sinensis" were grown in 800 mL volumes in 1 L Duran bottles incubated statically in the dark at 37°C. *Nitrosomonas europaea* ATCC19718 was obtained from the University of Aberdeen culture collection and cultivated in 200 mL volumes, in 500 mL conical flasks, shaking (160 rpm) at 30°C in modified Skinner and Walker (62) medium (pH~7.5) containing $(NH_4)_2SO_4$, 0.235 g L^{-1}; KH_2PO_4, 0.2 g L^{-1}; $CaCl_2$.$2H_2O$, 0.04 g L^{-1}; MgSO .$7H_2O$, 0.04 g L^{-1}, FeNaEDTA, 0.3 mg L^{-1}, buffered with 10 mM HEPES (pH 7.5) and 5% (w/v) Na_2CO_3. *Methylococcus capsulatus* (Bath) was grown in 50 mL volumes in 250 mL Quickfit conical flasks, shaking (180 rpm) at 37°C in nitrate mineral salts (NMS) supplemented with 20 µM copper to promote pMMO expression and under a CH_4 atmosphere of 40%. To confirm that *M. capsulatus* cells were only expressing pMMO and not sMMO, the naphthalene assay, which is specific for sMMO activity, was used (63) with sMMO-expressing *Methylocella silvestris* cells as positive controls.

Nitrite assay. NO_2^- concentrations were determined colorimetrically in a 96-well format using Griess reagent as previously described (60). Absorbance measurements were performed at 540 nm wavelength using a VersaMax Microplate Reader (Molecular Devices).

Inhibition of whole cells by alkynes. "*Ca.* Nitrosocosmicus franklandus" and "*Ca.* Nitrosotalea sinensis" were cultivated to mid-exponential phase (~600 – 700 µM and ~80 – 90 µM NO_2^- accumulated, respectively) and 1600 mL harvested by filtration onto nucleopore 0.2 µm membrane filters (PALL). "*Ca.* Nitrosocosmicus franklandus" cells were washed and

179 resuspended in 200 mL 10 mM HEPES (pH 7) buffered FWM salts to ~2 × 10^7 cells/mL. "*Ca.*
180 Nitrosotalea sinensis" cells were washed and resuspended in 100 mL 2.5 mM MES (pH 5.3)
181 buffered FWM salts to ~3 × 10^7 cells/mL. *N. europaea* was grown to mid-exponential phase and
182 400 mL culture was harvested by filtration, washed and resuspended to ~3 × 10^7 cells/mL in 200
183 mL 50 mM sodium phosphate buffer (pH 7.7), containing 2 mM $MgCl_2$ (12). *M. capsulatus* were
184 grown to an OD_{540} of 0.8 and 100 mL was harvested by centrifugation (14, 000 × *g*, 10 min).
185 Cells were washed and resuspended in 50 mL 10 mM PIPES buffer (pH 7) to ~2 × 10^8 cells/mL.
186 Cells were rested for 1 hour at their respective growth temperatures to achieve a baseline for
187 enzyme activity assays. Aliquots of 5 mL "*Ca.* Nitrosocosmicus franklandus", *N. europaea* and
188 *M. capsulatus* and 4 mL "*Ca.* Nitrosotalea sinensis" cell suspension were added to acid-washed
189 23 mL glass vials which were then sealed with grey butyl rubber stoppers, which had been
190 autoclaved two times to remove contaminating substances. C_2-C_8 linear 1-alkynes were added to
191 the headspace as vapour to achieve 10 µM aqueous concentration (C_{aq}), calculated using the
192 Henry's Law coefficients obtained from Sander (64). Phenylacetylene was dissolved in 100 %
193 dimethyl sulfoxide (DMSO) to achieve various stock solutions. A final volume of 5 µL stock
194 solution was added to cell suspensions resulting in 0.1% (v/v) DMSO plus the desired
195 concentration of phenylacetylene. Preliminary experiments determined the addition of 0.1% (v/v)
196 DMSO did not affect NH_4^+ oxidising activity (data not shown) and control treatments containing
197 0.1% (v/v) DMSO without phenylacetylene or acetylene were included. Cells were pre-incubated
198 with inhibitors for 30 minutes, to allow for the gas-liquid phase partitioning of the alkynes, at
199 37°C for "*Ca.* Nitrosocosmicus franklandus", "*Ca.* Nitrosotalea sinensis" and *M. capsulatus* and
200 at 30°C for *N. europaea*. Total inorganic ammonium (NH_3 + NH_4^+), referred to as NH_4^+, was
201 then added as NH_4Cl or $(NH_4)_2SO_4$ (reflecting the growth medium) to initiate NH_3 oxidising
202 activity and vials were incubated at the respective growth temperatures of the microorganisms.

M. capsulatus was incubated with shaking (150 rpm). AMO and pMMO activity was determined by assaying NO_2^- production from NH_3 oxidation in whole cells. NO_2^- production was measured and quantified as described above by withdrawing a sample of culture through the septum every 15 minutes for 2 hours unless otherwise stated. All treatments were carried out in triplicate and experiments were performed at least three times with similar results.

Sensitivity of isolates to C_2 to C_8 1-alkynes. C_2-C_8 linear 1-alkynes were added to vials using a gas tight syringe. To initiate NH_3 oxidation by "*Ca.* Nitrosocosmicus franklandus", *N. europaea* and "*Ca.* Nitrosotalea sinensis", NH_4^+ was added to a concentration of 1 mM by injection through the septum. For *M. capsulatus* (Bath), sodium formate was added first, as a source of reductant, immediately followed by NH_4^+, both at a final concentration of 20 mM.

Sensitivity of "*Ca.* Nitrosocosmicus franklandus" and *N. europaea* to phenylacetylene. Phenylacetylene was added to achieve concentrations ranging from 2.5 – 20 µM for "*Ca.* Nitrosocosmicus franklandus" and 0.5 – 10 µM for *N. europaea*. To initiate ammonia oxidation, NH_4^+ was added to a final concentration of 0.5 mM and 5 mM to "*Ca.* Nitrosocosmicus franklandus" and *N. europaea*, respectively. NO_2^- production was measured for 60 minutes.

Kinetic relationship between NH_4^+ and phenylacetylene inhibition of "*Ca.* Nitrosocosmicus franklandus" and *N. europaea.* To determine NH_3 oxidation kinetics in the presence of phenylacetylene, "*Ca.* Nitrosocosmicus franklandus" and *N. europaea* cells were harvested and resuspended as described above, but to a final concentration of 1×10^7 and 8×10^6 cells/mL, respectively. "*Ca.* Nitrosocosmicus franklandus" cell suspensions were pre-incubated with phenylacetylene (0, 4 or 8 µM) or acetylene (0 or 3 µM) for 30 minutes before the addition of various concentrations of NH_4^+ (0.005 - 1 mM). *N. europaea* cell suspensions were pre-

incubated with phenylacetylene (0, 0.2 or 0.4 µM) before the addition of 0.05 - 10 mM NH_4^+. Additional experiments were carried out to test the effect of 0.1% (v/v) DMSO on NH_3 oxidation kinetics by "*Ca.* Nitrosocosmicus franklandus" and *N. europaea* (Supplementary information Table S1).

Phenylacetylene inhibition of hydroxylamine oxidation by "*Ca.* Nitrosocosmicus franklandus". "*Ca.* Nitrosocosmicus franklandus" cell suspensions were incubated with 0 or 100 µM phenylacetylene. Hydroxylamine was added at a concentration of 200 µM and hydroxylamine-dependent NO_2^- production was measured over 60 minutes as described above.

Recovery of AMO activity from "*Ca.* Nitrosocosmicus franklandus" following phenylacetylene inhibition. "*Ca.* Nitrosocosmicus franklandus" cells were grown to mid-exponential phase and 3200 mL was harvested by filtration as described above and concentrated into 70 mL FWM containing 10 mM HEPES (pH 7.5). Aliquots of 5 mL cell suspension were added to glass vials and sealed with butyl rubber seals. Phenylacetylene (100 µM) and 1-octyne (200 µM) were added from DMSO stock solutions (as described above) and acetylene (20 µM) was added from a 1% (v/v in air) gaseous stock. Both control and acetylene treatments also contained 0.1% (v/v) DMSO. The addition of NH_4^+ (1 mM) initiated NH_3-oxidising activity and vials were incubated at 37°C overnight (16 hours). NO_2^- production was monitored for 1 hour to assess baseline activity. To remove inhibitors and test AMO recovery, samples were pooled into 50 mL Falcon tubes and the cells were washed three times in FWM containing 10 mM HEPES (pH 7.5) by centrifugation (12, 000× g for 10 minutes at 5°C). The pellet was resuspended in 700 µL FWM containing 10 mM HEPES (pH 7.5). Aliquots (200 µL) of cell suspension were added to 4.8 mL FWM containing 10 mM HEPES (pH 7.5) + 1 mM NH_4^+, resulting in a final cell

concentration of ~1.3 × 10^7 cells/mL. Vials were incubated in a water-bath (37°C) and NO_2^- production was monitored over 24 h.

Statistics. Linear 1-alkyne data were plotted as average activity as a fraction of the control treatments (no inhibitor). To analyse phenylacetylene inhibition kinetics, the initial rates of NO_2^- production were plotted against NH_4^+ concentration. A nonlinear regression was used to estimate the $K_{m(app)}$ and $V_{max(app)}$ for NH_4^+ using the Hyper32 kinetics package. Significant differences between treatments were identified by one-way ANOVA with Dunnett (2-sided) post-hoc test (IBM SPSS version 25).

Data Availability. The authors declare that the data supporting the findings of this study are available within the article [and its supplementary information file]. The AOA strains "*Ca.* Nitrosocosmicus franklandus" and "*Ca.* Nitrosotalea sinensis" are available from the corresponding author upon request.

Results

Sensitivity of "*Ca.* Nitrosocosmicus franklandus", "*Ca.* Nitrosotalea sinensis", *N. europaea* and pMMO-expressing *M. capsulatus* (Bath) to C_2 to C_8 1-alkynes

The sensitivity of intact "*Ca.* Nitrosocosmicus franklandus" and "*Ca.* Nitrosotalea sinensis" cells to 10 µM $C_{(aq)}$ C_2-C_8 1-alkynes was compared with the *N. europaea* and the pMMO-expressing methanotroph, *M. capsulatus* (Fig. 1). NH_3-dependent NO_2^- production by both "*Ca.* Nitrosocosmicus franklandus" and "*Ca.* Nitrosotalea sinensis" was inhibited by C_2-C_5 1-alkynes ($p < 0.001$) but not by C_7 and C_8 (Fig. 1 A and B). "*Ca.* Nitrosotalea sinensis" was strongly inhibited by C_4 and C_5 alkynes (degree of inhibition 54% ± 5% and 70% ± 1%,

respectively, compared with controls), however, these alkynes effected only partial inhibition of NH_3 oxidation by "*Ca.* Nitrosocosmicus franklandus" (24% ± 2% and 14% ± 1%, respectively), indicating differences in the alkyne sensitivities of different AOA strains. Additionally, C_6 had a significant inhibitory effect on "*Ca.* Nitrosotalea sinensis" ($p = 0.004$) but not on "*Ca.* Nitrosocosmicus franklandus" ($p = 0.47$). NO_2^- production by *N. europaea* was strongly inhibited by all 1-alkynes tested (C_2-C_8). 1-pentyne resulted in 98% ± 1% inhibition and AMO activity was completely inhibited by C_6-C_8 1-alkynes (Fig. 1C). In the presence of C_3 and C_4 1-alkynes, inhibition decreased to 78% ± 1% and 54% ± 1%, respectively. pMMO-expressing *M. capsulatus* cells oxidised NH_4^+ to NO_2^- and NO_2^- production was significantly inhibited by C_2-C_7 1-alkynes ($p \leq 0.001$), but C_6 and C_7 1-alkynes resulted in only approximately 10% inhibition compared with the control (Fig. 1D). NO_2^- production from NH_3 by the pMMO from *M. capsulatus* is shown in the supplementary information (Supplementary information Fig. S1). The rate of NO_2^- production decreased after 1 hour of incubation, likely due to the toxic build-up of NO_2^- and hydroxylamine in the culture.

Notably, "*Ca.* Nitrosotalea sinensis", *N. europaea* and *M. capsulatus* (Bath) were very sensitive to 10 µM acetylene (C_2) with NO_2^- production inhibited by >95 %, however, "*Ca.* Nitrosocosmicus franklandus" appeared less sensitive to acetylene (degree of inhibition, 82% ± 3%).

Inhibition of NO_2^- production by "*Ca.* Nitrosocosmicus franklandus" and *N. europaea* in response to phenylacetylene

Given the contrasting responses of ammonia oxidising archaea and bacteria to linear alkynes, AMO activity in the presence of the aromatic alkyne phenylacetylene was examined in "*Ca.* Nitrosocosmicus franklandus" and *N. europaea* cells (Fig. 2). After 1-hour of incubation,

293 the rate of NH_3-dependent NO_2^- production by "*Ca.* Nitrosocosmicus franklandus" was inhibited
294 by 55.4% ± 1.4% in the presence of 5 µM phenylacetylene compared to the DMSO control.
295 Incubations in the presence of 10 and 20 µM phenylacetylene increased the inhibition to 74.7% ±
296 0.5% and 86.0% ± 0.4%, respectively (Fig. 2A). NO_2^- production by *N. europaea* was inhibited
297 by 52.5% ± 1.7% in the presence of 0.5 µM phenylacetylene and, unlike the results from Lontoh
298 *et al.,* (54), who showed full inhibition at 0.6 µM, there was still partial NH_3-oxidising activity in
299 the presence of 1 µM phenylacetylene (75.1% ± 1.6% inhibition on the rate of NO_2^- production)
300 (Fig. 2B). Together, the results show that "*Ca.* Nitrosocosmicus franklandus" is approximately
301 10 × more resistant to phenylacetylene inhibition compared to *N. europaea.* Both "*Ca.*
302 Nitrosocosmicus franklandus" and *N. europaea* cells treated with 0.1 % DMSO produced NO_2^- at
303 a similar rate to untreated controls.

304 **Kinetic analysis of phenylacetylene inhibition of NH_4^+-dependent NO_2^- production by "*Ca.***
305 **Nitrosocosmicus franklandus" and *N. europaea***

306 To investigate the mode of inhibition of phenylacetylene on AMO, the initial reaction
307 velocity of NO_2^- production by "*Ca.* Nitrosocosmicus franklandus" and *N. europaea* were
308 determined over a range of substrate (total NH_4^+) concentrations. The concentrations of
309 phenylacetylene used in the kinetic analysis were selected to achieve partial inhibition of NO_2^-
310 production (Fig. 2). NH_3-dependent kinetics of initial NO_2^- production followed Michaelis-
311 Menten-type saturation kinetics for both "*Ca.* Nitrosocosmicus franklandus" and *N. europaea*
312 (Fig. 3A & B), where the velocity (v) of the AMO-catalysed reactions was hyperbolically related
313 to total NH_4^+ concentration ([S]) (Eq. 1):

314 (1)

$$v = \frac{V_{max}.[S]}{(K_m + [S])}$$

Apparent half-saturation constants for total NH_4^+ ($K_{m(app)}$) and maximum velocities ($V_{max(app)}$) in the presence/absence of phenylacetylene were calculated using hyperbolic regression analysis. The hyperbolic plots show that increasing the NH_4^+ concentration did not alleviate the inhibitory effect of phenylacetylene on NO_2^- production in "*Ca.* Nitrososcosmicus franklandus" or *N. europaea* (Fig. 3A & B). This suggests that phenylacetylene is not a simple competitive inhibitor of either the archaeal or the bacterial AMO with respect to NH_3 oxidation. Interestingly, the mechanism of inhibition by phenylacetylene appears to be different between "*Ca.* Nitrososcosmicus franklandus" and *N. europaea*. With "*Ca.* Nitrososcosmicus franklandus", the presence of 4 and 8 µM phenylacetylene decreased the $V_{max(app)}$ of NO_2^- production from 64.1 ± 2.6 nmol mg $prot^{-1}$ min^{-1} to 33.8 ± 2.2 and 20.1 ± 0.5 nmol mg $prot^{-1}$ min^{-1}, respectively (Table 1). There was no significant change in the $K_{m(app)}$ for cells inhibited by phenylacetylene compared to the control (p = 0.503 and p = 0.526, for 4 and 8 µM phenylacetylene, respectively), indicating that phenylacetylene and NH_3 do not compete for the same binding site. Inhibition of *N. europaea* by 0.2 and 0.4 µM phenylacetylene reduced both the $K_{m(app)}$ and the $V_{max(app)}$ by approximately 30 and 40%, respectively (Table 1). This is indicative of uncompetitive inhibition and suggests that phenylacetylene binds to the AMO subsequent to NH_3 binding and at a different binding site.

Previously, acetylene was shown to be a competitive inhibitor of the archaeal AMO from *Nitrososphaera viennensis* (48). To examine if acetylene interacts competitively with "*Ca.* Nitrososcosmicus franklandus" AMO, the kinetic response of NH_3-dependent NO_2^- production by "*Ca.* Nitrososcosmicus franklandus" to 3 µM acetylene was tested using the same experimental

design used to investigate phenylacetylene inhibition. In contrast to phenylacetylene, increasing the total NH_4^+ availability reduced acetylene inhibition, demonstrating that acetylene and NH_3 compete for the same AMO binding site (Supplementary information Fig. S2). Additionally, the $K_{m(app)}$ increased dramatically from 18.5 ± 2.9 µM to 691.3 ± 158.1 µM NH_4^+ in the presence of 3 µM acetylene, but there was no change in the $V_{max(app)}$ (Supplementary information Table S2), also demonstrating that acetylene interacts with the NH_3-binding site and decreases the affinity of the AMO for NH_3.

Phenylacetylene was dissolved in 100% DMSO and all cell suspensions used in both the phenylacetylene and acetylene experiments contained 0. 1% (v/v) DMSO. Therefore the addition of 0.1% (v/v) DMSO on NH_3 oxidation kinetics was tested separately. DMSO had no effect on kinetics parameters for NH_3 oxidation by "*Ca.* Nitrosocosmicus franklandus". For *N. europaea*, the presence of 0.1% (v/v) DMSO reduced the $K_{m(app)}$ and $V_{max(app)}$ by approximately 10% (Supplementary information Table S1).

The effect of phenylacetylene on hydroxylamine oxidation by "*Ca.* Nitrosocosmicus franklandus"

Hydroxylamine is the product of NH_3 oxidation by both the archaeal and bacterial AMO and is subsequently oxidised to other intermediates in the NO_2^- production pathway (65, 66). In order to verify that the reduction in the rate of NO_2^- production by "*Ca.* Nitrosocosmicus franklandus" was due to inhibition of NH_3 oxidation, rather than the effects of downstream enzymatic reactions, we investigated hydroxylamine oxidation by "*Ca.* Nitrosocosmicus franklandus" in the presence of phenylacetylene. NO_2^- production by "*Ca.* Nitrosocosmicus franklandus" was unaffected by 100 µM phenylacetylene relative to the DMSO control treatment, demonstrating that phenylacetylene is likely a specific inhibitor of the AMO from

359 "*Ca.* Nitrosocosmicus franklandus" (Fig. 4). Hydroxylamine-dependent NO_2^- production
360 proceeded rapidly but ceased after 30 minutes when approximately 27 µM NO_2^- had
361 accumulated. A similar response was previously observed for the marine AOA *Nitrosopumilus*
362 *maritimus* SCM1 (65).

363 **Recovery of AMO activity in "*Ca.* Nitrosocosmicus franklandus" following phenylacetylene**
364 **inhibition**

365 In order to establish whether phenylacetylene is a reversible or irreversible inhibitor of
366 AMO of "*Ca.* Nitrosocosmicus franklandus", the recovery of NH_3-oxidising activity after
367 exposure to phenylacetylene was investigated. Previous work has shown that in order to restore
368 AMO activity following inhibition by an irreversible inhibitor, for example acetylene, cells need
369 to synthesize new AMO enzyme which results in a lag phase before activity resumes (42). "*Ca.*
370 Nitrosocosmicus franklandus" cells were inhibited overnight by 100 µM phenylacetylene in the
371 presence of 1 mM NH_4^+. Since it was previously shown that inhibition by 1-octyne was
372 reversible in the AOA *N. viennensis*, in contrast to the irreversible action of acetylene (48),
373 treatments with both 1-octyne and acetylene were included as controls. To ensure that the
374 inability of cells to respond to substrate addition (NH_4^+) was not due to the effects of starvation,
375 controls incubated for a similar amount of time without either inhibitor or NH_4^+ were included
376 (starved cells). After the removal of the inhibitors by washing, cells were resuspended in NH_4^+-
377 replete medium. NO_2^- production, the proxy for NH_3 oxidation, by "*Ca.* Nitrosocosmicus
378 franklandus" recovered immediately following removal of 1-octyne. Cells inhibited by either
379 acetylene or phenylacetylene had a 3 to 5-hour lag time before NO_2^- production began,
380 suggesting that cells required *de novo* synthesis of new AMO in order to oxidise NH_3 (Fig. 5).
381 The starved cells recovered at the same rate as the controls (data not shown).

382 Cycloheximide is a potent inhibitor of protein synthesis in eukaryotes (67) and might be
383 expected to have a similar effect in archaea. Previously, Vajrala *et al.*, (68) demonstrated that it
384 inhibited protein synthesis in the marine AOA, *N. maritimus* SCM1, preventing the recovery of
385 NH_3-oxidising activity following inactivation of the AMO by acetylene. However, the same
386 concentration range of cycloheximide did not prevent the recovery of NH_3-oxidising activity in
387 *N. viennensis* following AMO inactivation with acetylene (48). Here, we observed that after
388 complete inhibition by 20 μM acetylene, cycloheximide slowed, although it did not completely
389 prevent, recovery of NH_3-oxidising activity by "*Ca.* Nitrosocosmicus franklandus"
390 (Supplementary information Fig. S3).

391 **Discussion**

392 **The inhibition of AMO and pMMO by linear alkynes**

393 Linear terminal alkynes have previously been shown to differentially inhibit archaeal and
394 bacterial AMO activity (47, 48). In agreement with this, NH_3-dependent NO_2^- production by the
395 AOA strains "*Ca.* Nitrosocosmicus franklandus" and "*Ca.* Nitrosotalea sinensis" was
396 considerably less sensitive to inhibition by longer-chain-length 1-alkynes ($\geq C_6$) compared to *N.*
397 *europaea* (Fig. 1). The linear 1-alkyne inhibition profile appears to be conserved across AOA
398 lineages with the overall trend of increased sensitivity to short-chain alkynes and reduced
399 sensitivity to longer-chain-length alkynes. This could indicate that, unlike the AMO from *N.*
400 *europaea*, the binding cavity of the archaeal AMO cannot orientate and activate larger linear
401 hydrocarbons such as 1-octyne, potentially due to steric hindrance caused by the bulkiness of
402 these substrates or inhibitors. Interestingly, inhibition of the AMO from "*Ca.* Nitrosocosmicus
403 franklandus" by 1-octyne, when used at 200 μM, was reversible and recovery of NH_3-oxidising

activity began immediately after removal of the inhibitor (Fig. 5). Similarly, Taylor *et al.*, (48) showed the inhibition of AMO from *N. viennensis* by 1-octyne was also reversible.

In contrast with AOA, NH_3 oxidation by *N. europaea* was fully or partially inhibited by all C_2-C_8 1-alkynes, with full inhibition occurring in the presence of longer-chain-length alkynes ($\geq C_6$). This is consistent with previous results published by Hyman *et al.*, (21) and Taylor *et al.*, (47) who found that long-chain-length 1-alkynes inhibited AMO of *N. europaea* more effectively than short-chain 1-alkynes. Additionally, it was observed by Hyman *et al.*, (21) that the effectiveness of *n*-alkynes as inhibitors of AMO from *N. europaea* inversely reflects the oxidation rate of *n*-alkanes of increasing chain length. For example, 1-octyne inactivates *N. europaea* AMO more rapidly and effectively than shorter-chain-length 1-alkynes, however, the corresponding alkane, 1-octane, is oxidised more slowly and yields less product compared to short-chain alkanes (21).

The pMMO has a narrower hydrocarbon substrate range compared to the AMO of *N. europaea* but is capable of oxidising short-chain *n*-alkanes ($\leq C_5$) and alkenes ($\leq C_3$) to their respective alcohols and epoxides (17). The specific site where hydrocarbon oxidation takes place within the pMMO is unclear. Intriguingly, a hydrophobic cavity identified in proximity to the predicted tricopper site in the PmoA from *M. capsulatus* (Bath) was shown to be of sufficient size to accommodate hydrocarbons of up to five carbons in length (30, 69, 70). Correspondingly, here we found that C_2-C_5 alkynes inhibited the NH_3-oxidising activity of pMMO from *M. capsulatus* (Bath) by more than 20%, reflecting the predicted size of this pMMO binding cavity (Fig. 1D). The inhibition of the pMMO by longer-chain alkynes (C_6-C_8) has not previously been tested and we found that NH_3 oxidation by *M. capsulatus* (Bath) was marginally inhibited by C_6

426 and C_7 alkynes, indicating that the pMMO can interact with longer-chain-length hydrocarbons
427 than those already known to be substrates.

428 The effectiveness of C_2-C_8 linear 1-alkynes as inhibitors of NH_3 oxidation by the AOA
429 strains used in this study and in previous studies (47, 48) indicates that the archaeal AMO has a
430 narrower hydrocarbon substrate range compared to the AMO of *N. europaea*. Furthermore, in
431 terms of the 1-alkyne inhibition profile, the AMO of "*Ca.* Nitrosocosmicus franklandus" and
432 "*Ca.* Nitrosotalea sinensis" more closely resembles the pMMO from *M. capsulatus* (Bath) than
433 the AMO of *N. europaea*. It could therefore be anticipated that the archaeal AMO oxidises a
434 similar range of linear *n*-alkanes and alkenes to that oxidised by the pMMO (Fig. 1).

435 Based on the diversity of archaeal AMO sequences (7), it is very likely that variation
436 exists between the structure and stereoselectivity of the AMO active site from different AOA
437 strains. Previously, Taylor *et al.*, (47, 48) observed differences in the sensitivity of *N. maritimus*,
438 *N. viennensis* and *Nitrososphaera gargensis* to inhibition by 1-hexyne (C_6) and 1-heptyne (C_7).
439 In this study, we did not observe significant inhibition of archaeal AMO activity by 1-heptyne,
440 although the AMO from "*Ca.* Nitrosotalea sinensis" was notably more sensitive to inhibition by
441 C_2-C_5 1-alkynes compared to AMO from "*Ca.* Nitrosocosmicus franklandus". Additionally, 1-
442 hexyne had a significant inhibitory effect on NO_2^- production by "*Ca.* Nitrosotalea sinensis" but
443 not by "*Ca.* Nitrosocosmicus franklandus" (Fig. 1A and B).

444 A considerable amount of research has focused on determining the environmental drivers
445 influencing AOA and AOB ecology and their relative contribution to nitrification.
446 Environmental factors, including substrate availability, pH, O_2 availability and temperature, have
447 been suggested to influence the ecological niche differentiation of ammonia oxidisers and to
448 control ammonia oxidation rates in distinct ecosystems. The resistance of "*Ca.* Nitrosocosmicus

449 franklandus" and "*Ca.* Nitrosotalea sinensis" to inhibition by 1-octyne (C_8) further justifies the
450 use of 1-octyne to distinguish between AOA and AOB nitrifying activity in soils and to reveal
451 the environmental factors influencing niche differentiation (49-51). Determining patterns in the
452 distribution of AOA and AOB in the environment could improve land and water management to
453 mitigate negative impacts associated with nitrification.

454

455 **The inhibition of AMO by phenylacetylene**

456 Evidence from field studies indicated that phenylacetylene inhibited nitrification activity
457 by AOA (53). Here, we examined phenylacetylene inhibition in pure culture with the terrestrial
458 AOA strain "*Ca.* Nitrosocosmicus franklandus". Our data show that in "*Ca.* Nitrosocosmicus
459 franklandus", phenylacetylene is a specific inhibitor of AMO, as it had no effect on
460 hydroxylamine-dependent NO_2^- production (Fig. 4). Kinetic analysis suggested that
461 phenylacetylene does not compete with NH_3 for the same AMO binding site, since increasing the
462 native substrate (NH_4^+) concentration did not protect against inhibition (Fig. 3A). In contrast,
463 higher concentrations of NH_4^+ did provide a protective effect when "*Ca.* Nitrosocosmicus
464 franklandus" was incubated with acetylene, indicating acetylene and NH_3 compete for the same
465 binding site (Supplementary information Fig. S2). The recovery of AMO activity following
466 complete inhibition by phenylacetylene incorporated a significant lag phase, similar to that
467 observed for acetylene, suggesting that inhibition by these alkynes was irreversible, and that cells
468 required *de novo* protein synthesis of new AMO to re-establish NH_4^+-oxidising activity (Fig. 5).
469 Irreversible inhibition could indicate that the binding cavity of the AMO from "*Ca.*
470 Nitrosocosmicus franklandus" is large enough to enable the orientation and subsequent activation
471 of phenylacetylene, and that phenylacetylene and acetylene essentially both act as suicide

472 substrates. Curiously though, our data suggest that phenylacetylene does not interact with the
473 same binding site on the AMO as NH_3 and acetylene.

474 Phenylacetylene is an irreversible inhibitor of AMO from *N. europaea* (41, 46). Here we
475 demonstrate that phenylacetylene does not compete with NH_3 for the same binding site (Fig. 3B).
476 It has been proposed that the AMO from *N. europaea* may contain two distinct binding sites, one
477 that specifically binds NH_3 and hydrocarbons $\leq C_3$ and a second that binds larger hydrocarbons,
478 with oxidation occurring at either site (23, 45). Alternatively, different hydrocarbons might be
479 able to access the active site of the AMO from two different directions (45). pMMO-expressing
480 methanotrophs also exhibit complicated inhibition patterns when exposed to multiple
481 hydrocarbon substrates. For example, dichloromethane acted as a competitive inhibitor of
482 methane oxidation by *Methylosinus trichosporium* OB3b, but trichloromethane was best
483 described as a noncompetitive inhibitor, suggesting the existence of at least two substrate binding
484 sites (20). Although the location and nuclearity of the active site for methane oxidation is still
485 under debate, it is generally accepted that the pMMO contains multiple metal-binding sites, or
486 potential active sites, and therefore it is possible that different hydrocarbons are oxidised at
487 distinct sites on the pMMO. The non-competitive nature of phenylacetylene inhibition, with
488 respect to NH_3, of the AMO from "*Ca.* Nitrosocosmicus franklandus" provides early indications
489 that distinct binding sites may be present on the archaeal AMO, or that there are two separate
490 routes by which substrates can access the archaeal AMO active site.

491 Kinetic analysis of phenylacetylene inhibition of AMO of "*Ca.* Nitrosocosmicus
492 franklandus" and *N. europaea* revealed that phenylacetylene most likely interacts with the AMOs
493 via distinct mechanisms. Specifically, phenylacetylene inhibition of AMO from *N. europaea* had
494 characteristics of uncompetitive inhibition, where both the $K_{m(app)}$ and $V_{max(app)}$ decreased with

increasing concentrations of phenylacetylene, indicating that the inhibitor only has affinity for the enzyme-substrate complex. Potentially, the binding of NH_3 induces a structural change in the AMO binding cavity, enabling phenylacetylene to bind at a putative secondary (non-NH_3) site. Phenylacetylene inhibition of the AMO from "*Ca.* Nitrosocosmicus franklandus" did not show the same characteristics as in *N. europaea* (Table 1), demonstrating that the interaction between phenylacetylene and the active site differed between the distinct AMO types.

Both AMO- and pMMO-expressing microorganisms have received interest for their potential use in bioremediation due to their capability to co-oxidize persistent organic pollutants such as halogenated alkanes and alkenes and chlorinated hydrocarbons (71, 72). Unlike the bacterial AMO, the oxidation of aromatic compounds has not been observed by the pMMO (17, 21, 45, and 56). Lontoh *et al.*, (54) showed that pMMO from *M. capsulatus* (Bath) and several other strains of methanotrophs were relatively resistant to phenylacetylene inhibition, with whole-cell pMMO activity still present at 1 mM phenylacetylene. It is possible that aromatic compounds are simply too bulky to gain access to or be orientated at the pMMO active site (69). Although *N. europaea* appears to lack the ability to completely mineralise aromatic pollutants, it may initiate degradation of aromatic compounds and provide oxidation products that can be transformed by other microorganisms (24). There is evidence that the archaeal AMO, unlike the pMMO, is capable of transforming aromatic compounds. Recently, Men *et al.*, (73) demonstrated that the AOA strain *N. gargensis* was capable of co-metabolising two tertiary amines, mianserin and ranitidine, with the initial oxidative reaction most likely carried out by the AMO. Given that AOA have a significantly higher substrate affinity than AOB (74), AOA might be more effective in the biotransformation of some organic pollutants.

This research offers new insights into the structure and substrate range of AMO from archaea using alkyne inhibitors, in comparison with other members of the CuMMO family. Future studies should investigate the inhibition and subsequent co-oxidation of potential archaeal AMO substrates. Examining alternative substrate reactions and products could provide information about archaeal AMO stereoselectivity, advance our understanding of the enzyme structure and improve predicted structural models for archaeal AMO.

Acknowledgements

L.E.L-M is funded by a Royal Society Dorothy Hodgkin Research Fellowship (DH150187). C.L.W is funded by a University of East Anglia funded PhD studentship. A.S is funded by a Royal Society Dorothy Hodgkin Fellowship Enhancement Award (RGF\EA\180300). A.T.C is funded by a Leverhulme Trust Early Career Fellowship (ECF-2016-626).

We thank Dr Tom Clarke for valuable discussion on the analysis of the kinetics data.

References

1. Daims H, Lebedeva EV, Pjevac P, Han P, Herbold C, Albertsen M, Jehmlich N, Palatinszky M, Vierheilig J, Bulaev A, Kirkegaard RH, von Bergen M, Rattei T, Bendinger B, Nielsen PH, Wagner M. 2015. Complete nitrification by *Nitrospira* bacteria. *Nature* 528:504-509.
2. Van Kessel MA, Speth DR, Albertsen M, Nielsen PH, den Camp HJO, Kartal B, Jetten MS, Lücker S. 2015. Complete nitrification by a single microorganism. *Nature* 528:555-559.

3. Lehtovirta-Morley LE. 2018. Ammonia oxidation: Ecology, physiology, biochemistry and why they must all come together. *FEMS Microbiol Lett* 365:fny058.
4. Leininger S, Urich T, Schloter M, Schwark L, Qi J, Nicol GW, Prosser JI, Schuster SC, Schleper C. 2006. Archaea predominate among ammonia-oxidizing prokaryotes in soils. *Nature* 442:806-809.
5. Wuchter C, Abbas B, Coolen MJ, Herfort L, van Bleijswijk J, Timmers P, Strous M, Teira E, Herndl GJ, Middelburg JJ, Schouten S, Sinninghe Damsté JS. 2006. Archaeal nitrification in the ocean. *Proc Natl Acad Sci U S A* 103:12317-12322.
6. Francis CA, Beman JM, Kuypers MM. 2007. New processes and players in the nitrogen cycle: the microbial ecology of anaerobic and archaeal ammonia oxidation. *ISME J* 1:19-27.
7. Alves RJE, Minh BQ, Urich T, von Haeseler A, Schleper C. 2018. Unifying the global phylogeny and environmental distribution of ammonia-oxidising archaea based on *amoA* genes. *Nat Commu* 9:1517.
8. Lawton TJ, Ham J, Sun T, Rosenzweig AC. 2014. Structural conservation of the B subunit in the ammonia monooxygenase/particulate methane monooxygenase superfamily. *Proteins* 82:2263-2267.
9. Lancaster KM, Caranto JD, Majer SH, Smith MA. 2018. Alternative bioenergy: updates to and challenges in nitrification metalloenzymology. *Joule* 2:421-441.
10. Holmes AJ, Costello A, Lidstrom ME, Murrell JC. 1995. Evidence that participate methane monooxygenase and ammonia monooxygenase may be evolutionarily related. *FEMS Microbiol Lett* 132:203-208.
11. Pester M, Schleper C, Wagner M. 2011. The Thaumarchaeota: an emerging view of their phylogeny and ecophysiology. *Curr Opin Microbiol* 14:300-306.

12. Hyman MR, Wood PM. 1983. Methane oxidation by *Nitrosomonas europaea*. *Biochem J* 212:31-37.

13. Ward BB. 1987. Kinetic studies on ammonia and methane oxidation by *Nitrosococcus oceanus*. *Arch Microbiol* 147:126-133.

14. Dalton H. 1977. Ammonia oxidation by the methane oxidising bacterium *Methylococcus capsulatus* strain Bath. *Arch Microbiol* 114:273-279.

15. O'neill JG, Wilkinson JF. 1977. Oxidation of ammonia by methane-oxidizing bacteria and the effects of ammonia on methane oxidation. *J Gen Microbiol* 100:407-412.

16. Nyerges G, Stein LY. 2009. Ammonia cometabolism and product inhibition vary considerably among species of methanotrophic bacteria. *FEMS Microbiol Lett* 297:131-136.

17. Burrows KJ, Cornish A, Scott D, Higgins IJ. 1984. Substrate specificities of the soluble and particulate methane mono-oxygenases of *Methylosinus trichosporium* OB3b. *J Gen Microbiol* 130:3327-3333.

18. Bédard C, Knowles R. 1989. Physiology, biochemistry, and specific inhibitors of CH_4, NH_4^+, and CO oxidation by methanotrophs and nitrifiers. *Microbiol Mol Biol Rev* 53:68-84.

19. Miyaji A, Miyoshi T, Motokura K, Baba T. 2011. The substrate binding cavity of particulate methane monooxygenase from *Methylosinus trichosporium* OB3b expresses high enantioselectivity for n-butane and n-pentane oxidation to 2-alcohol. *Biotechnol Lett* 33:2241.

20. Lontoh S, DiSpirito AA, Semrau JD. (1999). Dichloromethane and trichloroethylene inhibition of methane oxidation by the membrane-associated methane monooxygenase of *Methylosinus trichosporium* OB3b. *Arch Microbiol* 171:301-308.

21. Hyman MR, Murton IB, Arp DJ. 1988. Interaction of ammonia monooxygenase from *Nitrosomonas europaea* with alkanes, alkenes, and alkynes. *Appl Environ Microbiol* 54:3187-3190.

22. Rasche ME, Hyman MR, Arp DJ. 1991. Factors limiting aliphatic chlorocarbon degradation by *Nitrosomonas europaea*: cometabolic inactivation of ammonia monooxygenase and substrate specificity. *Appl Environ Microbiol* 57:2986-2994.

23. Keener WK, Arp DJ. 1993. Kinetic studies of ammonia monooxygenase inhibition in *Nitrosomonas europaea* by hydrocarbons and halogenated hydrocarbons in an optimized whole-cell assay. *Appl Environ Microbiol* 59:2501-2510.

24. Keener WK, Arp DJ. 1994. Transformations of aromatic compounds by *Nitrosomonas europaea*. *Appl Environ Microbiol* 60:1914-1920.

25. Hyman MR, Kim CY, Arp DJ. 1990. Inhibition of ammonia monooxygenase in *Nitrosomonas europaea* by carbon disulfide. *J Bacteriol* 172:4775-4782.

26. Juliette LY, Hyman MR, Arp DJ. 1993. Inhibition of ammonia oxidation in *Nitrosomonas europaea* by sulfur compounds: thioethers are oxidized to sulfoxides by ammonia monooxygenase. *Appl Environ Microbiol* 59:3718-3727.

27. Lieberman RL, Rosenzweig AC. 2005. Crystal structure of a membrane-bound metalloenzyme that catalyses the biological oxidation of methane. *Nature* 434:177-182.

28. Walker CB, De La Torre JR, Klotz MG, Urakawa H, Pinel N, Arp DJ, Brochier-Armanet C, Chain PSG, Chan PP, Gollabgir A, Hemp J, Hügler M, Karr EA, Könneke M, Shin M, Lawton TJ, Lowe T, Martens-Habbena W, Sayavedra-Soto LA, Lang D, Sievert SM, Rosenzweig AC, Manning G, Stahl DA. 2010. *Nitrosopumilus maritimus* genome reveals unique mechanisms for nitrification and autotrophy in globally distributed marine crenarchaea. *Proc Natl Acad Sci* 107:8818-8823.

29. Martinho M, Choi DW, DiSpirito AA, Antholine WE, Semrau JD, Münck E. 2007. Mössbauer studies of the membrane-associated methane monooxygenase from *Methylococcus capsulatus* Bath: evidence for a diiron center. *J Am Chem Soc* 129:15783-15785.

30. Chan SI, Yu SSF. 2008. Controlled oxidation of hydrocarbons by the membrane-bound methane monooxygenase: The case for a tricopper cluster. *Acc Chem Res* 41:969-979.

31. Cao L, Caldararu O, Rosenzweig AC, Ryde U. 2018. Quantum refinement does not support dinuclear copper sites in crystal structures of particulate methane monooxygenase. *Angew Chem Int Ed Engl* 57:162-166.

32. Lu YJ, Hung MC, Chang BTA, Lee TL, Lin ZH, Tsai IK, Chen YS, Chang CS, Tsai YF, Chen KHC, Chan SI. 2019. The PmoB subunit of particulate methane monooxygenase (pMMO) in *Methylococcus capsulatus (*Bath): The CuI sponge and its function. *J Inorg Biochem* 196:110691.

33. Ross MO, MacMillan F, Wang J, Nisthal A, Lawton TJ, Olafson BD, Mayo SL, Rosenzweig AC, Hoffman BM. 2019. Particulate methane monooxygenase contains only mononuclear copper centers. *Science* 364:566-570.

34. Ro SY, Schachner LF, Koo CW, Purohit R, Remis JP, Kenney GE, Liauw BW, Thomas PM, Patrie SM, Kelleher NL, Rosenzweig AC. 2019. Native top-down mass spectrometry provides insights into the copper centers of membrane-bound methane monooxygenase. *Nature Commun* 10:2675

35. Hooper AB, Terry KR. 1973. Specific inhibitors of ammonia oxidation in *Nitrosomonas*. *J Bacteriol* 115:480-485.

633 36. Taylor AE, Zeglin LH, Dooley S, Myrold DD, Bottomley PJ. 2010. Evidence for
634 different contributions of archaea and bacteria to the ammonia-oxidizing potential of
635 diverse Oregon soils. *Appl Environ Microbiol* 76:7691-7698.
636 37. Lehtovirta-Morley LE, Verhamme DT, Nicol GW, Prosser JI. 2013. Effect of nitrification
637 inhibitors on the growth and activity of *Nitrosotalea devanaterra* in culture and soil. *Soil*
638 *Biol and Biochem* 62:129-133.
639 38. Shen T, Stieglmeier M, Dai J, Urich T, Schleper C. 2013. Responses of the terrestrial
640 ammonia-oxidizing archaeon *Ca*. Nitrososphaera viennensis and the ammonia-oxidizing
641 bacterium *Nitrosospira multiformis* to nitrification inhibitors. *FEMS Microbiol Lett*
642 344:121-129.
643 39. Hynes RK, Knowles R. 1982. Effect of acetylene on autotrophic and heterotrophic
644 nitrification. *Can J Microbiol* 28:334-340.
645 40. Prior SD, Dalton H. 1985. Acetylene as a suicide substrate and active site probe for
646 methane monooxygenase from *Methylococcus capsulatus* (Bath). *FEMS Microbiol Lett*
647 29:105-109.
648 41. Hyman MR, Wood PM. 1985. Suicidal inactivation and labelling of ammonia mono-
649 oxygenase by acetylene. *Biochem J* 227:719-725.
650 42. Hyman MR, Arp DJ. 1992. $^{14}C_2H_2$-and $^{14}CO_2$-labeling studies of the *de novo* synthesis of
651 polypeptides by *Nitrosomonas europaea* during recovery from acetylene and light
652 inactivation of ammonia monooxygenase. *J Biol Chem* 267:1534-1545.
653 43. McTavish HJ, Fuchs JA, Hooper AB. 1993. Sequence of the gene coding for ammonia
654 monooxygenase in *Nitrosomonas europaea*. *J Bacteriol* 175:2436-2444.

655 44. Gilch S, Vogel M, Lorenz MW, Meyer O, Schmidt I. 2009. Interaction of the
656 mechanism-based inactivator acetylene with ammonia monooxygenase of *Nitrosomonas*
657 *europaea*. *Microbiol* 155:279-284.
658 45. Keener WK, Russell SA, Arp DJ. 1998. Kinetic characterization of the inactivation of
659 ammonia monooxygenase in *Nitrosomonas europaea* by alkyne, aniline and
660 cyclopropane derivatives. *Biochim Biophys Acta* 1388:373-385.
661 46. Bennett K, Sadler NC, Wright AT, Yeager C, Hyman MR. 2016 Activity-based protein
662 profiling of ammonia monooxygenase in *Nitrosomonas europaea*. *Appl Environ*
663 *Microbiol* 82:2270–2279.
664 47. Taylor AE, Vajrala N, Giguere AT, Gitelman AI, Arp DJ, Myrold DD, Sayavedra-Soto
665 L, Bottomley PJ. 2013. Use of aliphatic n-alkynes to discriminate soil nitrification
666 activities of ammonia-oxidizing thaumarchaea and bacteria. *Appl Environ Microbiol*
667 79:6544-6551.
668 48. Taylor AE, Taylor K, Tennigkeit B, Palatinszky M, Stieglmeier M, Myrold DD, Schleper
669 C, Wagner M, Bottomley PJ. 2015. Inhibitory effects of C2 to C10 1-alkynes on
670 ammonia oxidation in two *Nitrososphaera* species. *Appl Environ Microbiol* 81:1942-
671 1948.
672 49. Lu X, Bottomley PJ, Myrold DD. 2015. Contributions of ammonia-oxidizing archaea and
673 bacteria to nitrification in Oregon forest soils. *Soil Biol Biochem* 85:54-62.
674 50. Taylor AE, Giguere AT, Zoebelein CM, Myrold DD, Bottomley PJ. 2017. Modeling of
675 soil nitrification responses to temperature reveals thermodynamic differences between
676 ammonia-oxidizing activity of archaea and bacteria. *ISME J* 11:896-908.

677 51. Giguere AT, Taylor AE, Suwa Y, Myrold DD, Bottomley PJ. 2017. Uncoupling of
678 ammonia oxidation from nitrite oxidation: impact upon nitrous oxide production in non-
679 cropped Oregon soils. *Soil Biol Biochem* 104:30-38.
680 52. Hink L, Nicol GW, Prosser JI. 2017. Archaea produce lower yields of N_2O than bacteria
681 during aerobic ammonia oxidation in soil. *Environ Microbiol* 19:4829-4837.
682 53. Im J, Lee SW, Bodrossy L, Barcelona MJ, Semrau JD. 2011. Field application of
683 nitrogen and phenylacetylene to mitigate greenhouse gas emissions from landfill cover
684 soils: effects on microbial community structure. *Appl Microbiol Biotechnol* 89:189-200.
685 54. Lontoh S, DiSpirito AA, Krema CL, Whittaker MR, Hooper AB, Semrau JD. 2000.
686 Differential inhibition *in vivo* of ammonia monooxygenase, soluble methane
687 monooxygenase and membrane-associated methane monooxygenase by phenylacetylene.
688 *Environ Microbiol* 2:485-494.
689 55. Vannelli T, Hooper AB. 1995. NIH shift in the hydroxylation of aromatic compounds by
690 the ammonia-oxidizing bacterium *Nitrosomonas europaea*. Evidence against an arene
691 oxide intermediate. *Biochem* 34:11743-11749.
692 56. Colby J, Stirling DI, Dalton, H. 1977. The soluble methane mono-oxygenase of
693 *Methylococcus capsulatus* (Bath). Its ability to oxygenate *n*-alkanes, *n*-alkenes, ethers,
694 and alicyclic, aromatic and heterocyclic compounds. *Biochem J* 165:395-402.
695 57. Campbell MA, Nyerges G, Kozlowski JA, Poret-Peterson AT, Stein LY, Klotz MG.
696 2011. Model of the molecular basis for hydroxylamine oxidation and nitrous oxide
697 production in methanotrophic bacteria. *FEMS Microbiol Lett* 322:82-89.
698 58. Suzuki I, Dular U, Kwok SC. 1974. Ammonia or ammonium ion as substrate for
699 oxidation by *Nitrosomonas europaea* cells and extracts. *J Bacteriol* 120:556-558.

59. Lehtovirta-Morley LE, Sayavedra-Soto LA, Gallois N, Schouten S, Stein LY, Prosser JI, Nicol GW. 2016. Identifying potential mechanisms enabling acidophily in the ammonia-oxidizing archaeon "*Candidatus* Nitrosotalea devanaterra". *Appl Environ Microbiol* 82:2608-2619.

60. Lehtovirta-Morley LE, Ge C, Ross J, Yao H, Nicol GW, Prosser JI. 2014. Characterisation of terrestrial acidophilic archaeal ammonia oxidisers and their inhibition and stimulation by organic compounds. *FEMS Microbiol Ecol* 89:542-552.

61. Lehtovirta-Morley LE, Ross J, Hink L, Weber EB, Gubry-Rangin C, Thion C, Prosser JI, Nicol GW. 2016. Isolation of '*Candidatus* Nitrosocosmicus franklandus', a novel ureolytic soil archaeal ammonia oxidiser with tolerance to high ammonia concentration. *FEMS Microbiol Ecol* 92: fiw057.

62. Skinner FA, Walker N. 1961. Growth of *Nitrosomonas europaea* in batch and continuous culture. *Arch Mikrobiol* 38:339-349.

63. Brusseau GA, Tsien HC, Hanson RS, Wackett LP. 1990. Optimization of trichloroethylene oxidation by methanotrophs and the use of a colorimetric assay to detect soluble methane monooxygenase activity. *Biodegrad* 1:19-29.

64. Sander R. 2015. Compilation of Henry's law constants (version 4.0) for water as solvent. *Atmos Chem Phys* 15:4399-4981.

65. Vajrala N, Martens-Habbena W, Sayavedra-Soto LA, Schauer A, Bottomley PJ, Stahl DA, Arp DJ. 2013. Hydroxylamine as an intermediate in ammonia oxidation by globally abundant marine archaea. *Proc Natl Acad Sci* 110:1006-1011.

66. Caranto JD, Lancaster KM. 2017. Nitric oxide is an obligate bacterial nitrification intermediate produced by hydroxylamine oxidoreductase. *Proc Natl Acad Sci* 114:8217-8222.

67. Siegel MR, Sisler HD. 1963. Inhibition of protein synthesis *in vitro* by cycloheximide. *Nature* 200:675.

68. Vajrala N, Bottomley PJ, Stahl DA, Arp DJ, Sayavedra-Soto LA. 2014. Cycloheximide prevents the *de novo* polypeptide synthesis required to recover from acetylene inhibition in *Nitrosopumilus maritimus*. *FEMS Microbiol Ecol* 88:495-502.

69. Ng KY, Tu LC, Wang YS, Chan SI, Yu SSF. 2008. Probing the hydrophobic pocket of the active site in the particulate methane monooxygenase (pMMO) from *Methylococcus capsulatus* (Bath) by variable stereoselective alkane hydroxylation and olefin epoxidation. *ChemBioChem* 9:1116-1123.

70. Culpepper MA, Rosenzweig AC. 2012. Architecture and active site of particulate methane monooxygenase. *Crit Rev Biochem Mol Biol* 47:483-492.

71. Sayavedra-Soto LA, Gvakharia B, Bottomley PJ, Arp DJ, Dolan ME. 2010. Nitrification and degradation of halogenated hydrocarbons—a tenuous balance for ammonia-oxidizing bacteria. *Appl Microbiology and Biotechnol* 86:435-444.

72. Semrau J. 2011. Bioremediation via methanotrophy: overview of recent findings and suggestions for future research. *Front Microbiol* 2:209.

73. Men Y, Han P, Helbling DE, Jehmlich N, Herbold C, Gulde R, Onnis-Hayden A, Gu AZ, Johnson DR, Wagner M, Fenner K. 2016. Biotransformation of two pharmaceuticals by the ammonia-oxidizing archaeon *Nitrososphaera gargensis*. *Environ Sci Technol* 50:4682-4692.

74. Martens-Habbena W, Berube PM, Urakawa H, de la Torre JR, Stahl DA. 2009. Ammonia oxidation kinetics determine niche separation of nitrifying Archaea and Bacteria. *Nature* 461:976-979.

748 **Table 1.** Kinetics of NH_3-dependent NO_2^- production by "*Ca.* Nitrosocosmicus franklandus" and

749 *N. europaea* in the presence of phenylacetylene. SE of three replicates are in parentheses (n=3).

750 For 0 µM phenylacetylene, SE is from two independent experiments (n=6).

Strain	Phenylacetylene (µM)	$K_{m(app)}$ (µM)	$V_{max(app)}$ (nmol mg $prot^{-1}$ min^{-1})
"*Ca.* Nitrosocosmicus franklandus"	0	26.7 (4.7)	64.1 (2.6)
	4	30.3 (8.3)	33.8 (2.2)
	8	22.9 (3.2)	20.1 (0.5)
N. europaea	0	520.3 (19.6)	324.4 (3.7)
	0.2	375.3 (17.4)	240.7 (2.7)
	0.4	318.4 (13.8)	188.7 (2.0)

751

752

753

754

755

756

757

758

759

760 **FIG 1** Inhibition of NO_2^- production by "*Ca.* Nitrosocosmicus franklandus" (A), "*Ca.*
761 Nitrosotalea sinensis" (B), *N. europaea* (C) and *M. capsulatus* (Bath) (D) in response to 10 µM
762 (C_{aq}) C_2- C_8 1-alkynes. *N. europaea*, "*Ca.* Nitrosocosmicus franklandus" and "*Ca.* Nitrosotalea
763 sinensis" were incubated with 1 mM NH_4^+ and *M. capsulatus* (Bath) with 20 mM NH_4^+. Error
764 bars represent standard error (SE) of the mean (n = 3). * Indicates 1-alkyne treatments that
765 significantly inhibited NO_2^- production relative to the control treatment ($p < 0.01$).

766 **FIG 2** NO_2^- production by "*Ca.* Nitrosocosmicus franklandus" (A) and *N. europaea* (B) in
767 response to different concentrations of phenylacetylene (PA) dissolved in DMSO. Error bars
768 representing SE are included but usually smaller than markers (n = 3).

769 **FIG 3** Michaelis-Menten hyperbolic plot showing the initial rate of NO_2^- production by "*Ca.*
770 Nitrosocosmicus franklandus" (A) and *N. europaea* (B) to phenylacetylene (PA) dissolved in
771 DMSO as a function of NH_4^+ concentration. The x-axis is the substrate (NH_4^+) concentration and
772 the y-axis is the initial rate of NO_2^- production. Inhibition was not overcome by increasing
773 concentration of NH_4^+, indicating that phenylacetylene and NH_3 do not compete for the same
774 binding site. Error bars represent SE (n = 3).

775 **FIG 4** NO_2^- production from hydroxylamine oxidation by "*Ca.* Nitrosocosmicus franklandus" in
776 the presence or absence of 100 µM phenylacetylene (PA) dissolved in DMSO. Error bars
777 represent SE (n = 3).

778 **FIG 5** Time course recovery of NO_2^- production by "*Ca.* Nitrosocosmicus franklandus"
779 following overnight inhibition of NH_3 oxidation by phenylacetylene (100 µM), acetylene (20
780 µM) and 1-octyne (200 µM). Error bars represent SE (n = 3).

Figure 1

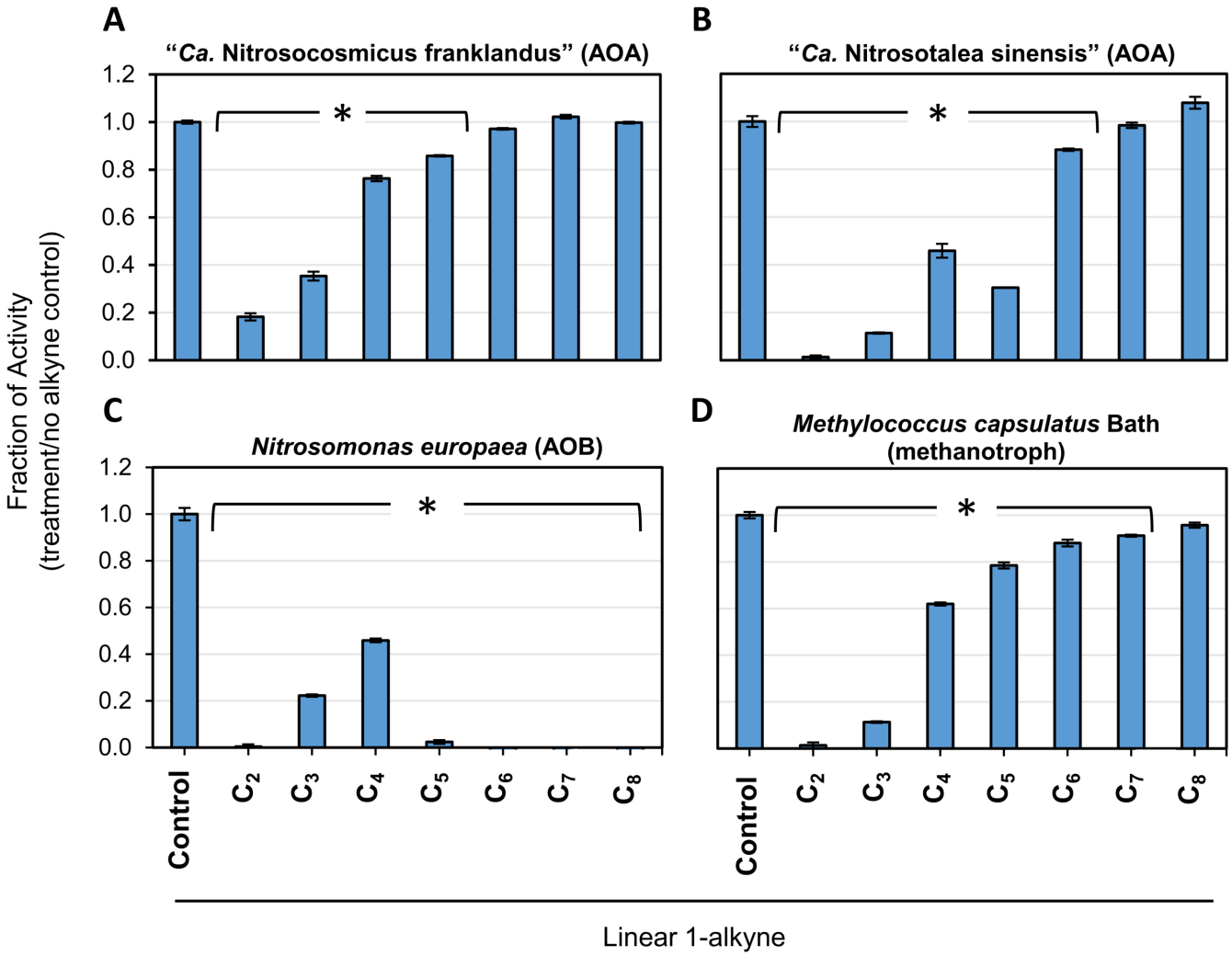

Figure 2

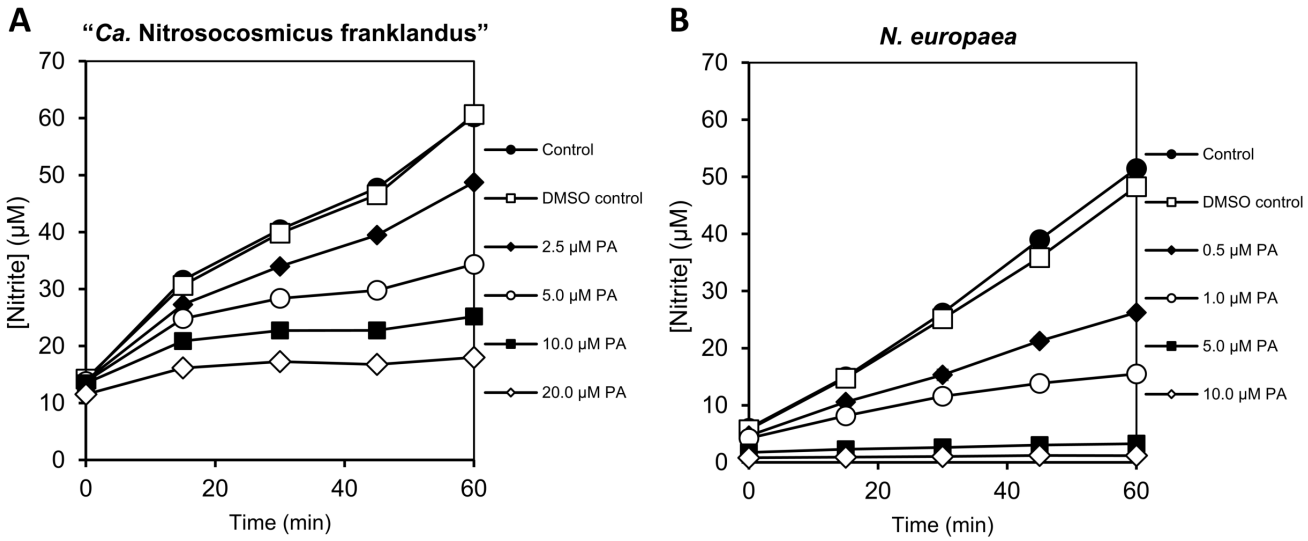

Figure 3

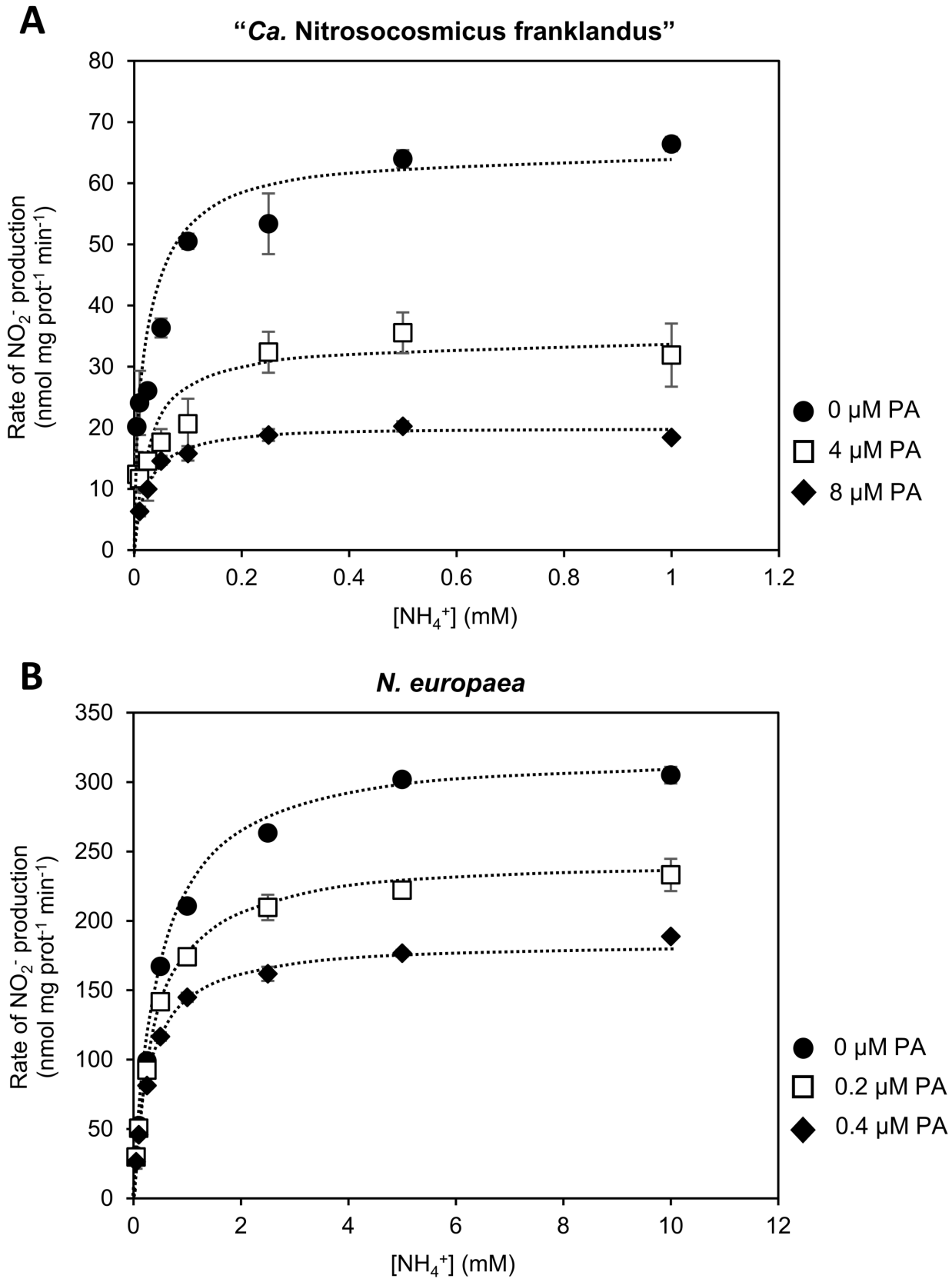

Figure 4

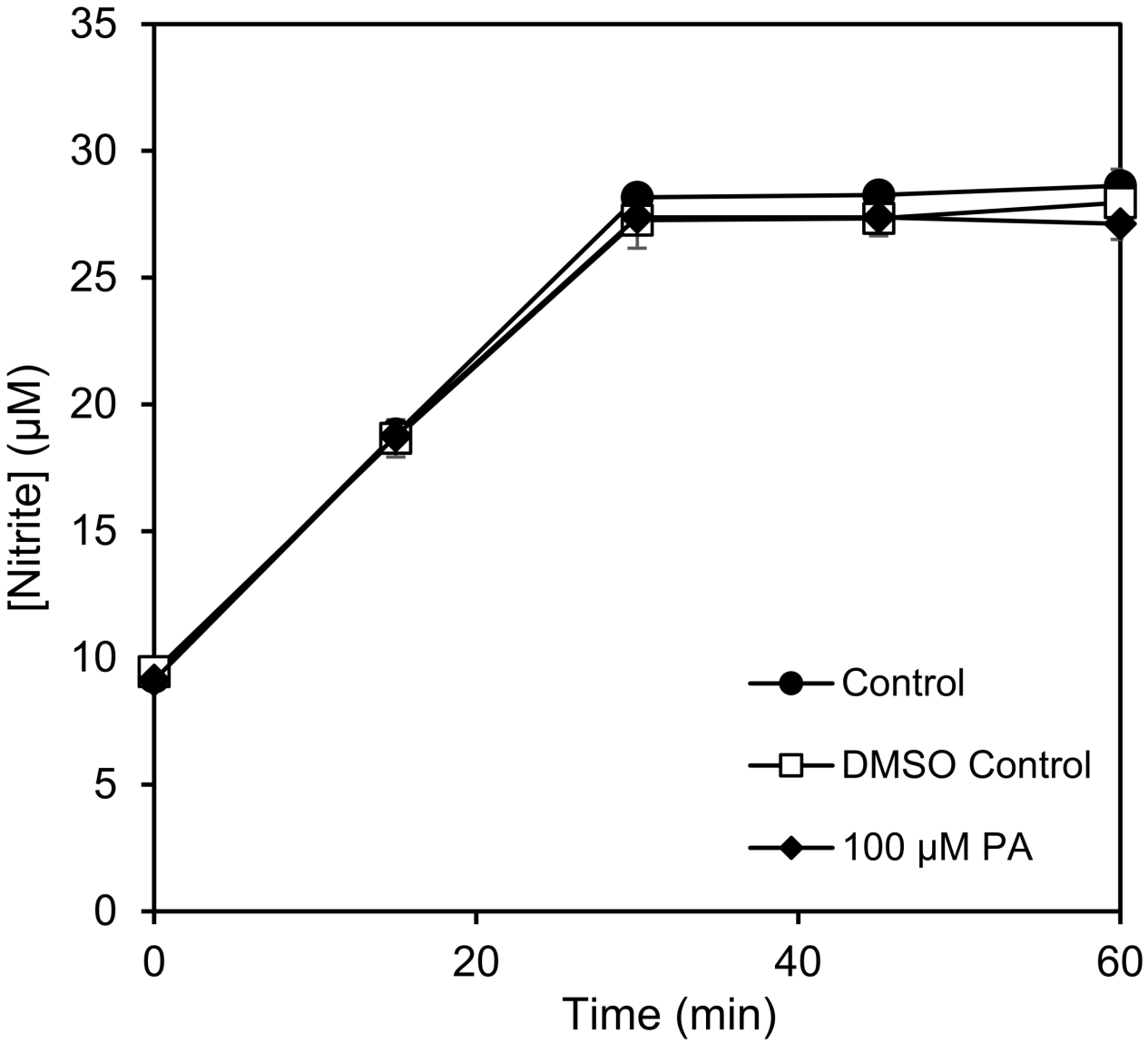

Figure 5